

# Ultraviolet-to-Far Infrared Properties of Lyman Break Galaxies and Luminous Infrared Galaxies at $z \sim 1$

D. Burgarella<sup>1</sup>, Pablo G. Pérez-González<sup>2</sup>, K. Crystal D. Tyler<sup>2</sup>, George H. Rieke<sup>2</sup>, Veronique Buat<sup>1</sup>,  
Tutomu T. Takeuchi<sup>1,10</sup>, Sébastien Lauger<sup>1</sup>, Stéphane Amouts<sup>1</sup>, Olivier Ilbert<sup>3</sup>, Tom A. Barlow<sup>4</sup>, Luciana  
Bianchi<sup>5</sup>, Young-Wook Lee<sup>6</sup>, Barry F. Madore<sup>7,8</sup>, Roger F. Malina<sup>1</sup>, Alex S. Szalay<sup>9</sup> and Sukyoung K. Yi<sup>6</sup>

<sup>1</sup> Observatoire Astronomique Marseille Provence, Laboratoire d'Astrophysique de Marseille, traverse du siphon, 13376 Marseille cedex 12, France

e-mail: denis.burgarella@; veronique.buat@; tutomu.takeuchi@; sebastien.lauger@oamp.fr

<sup>2</sup> Steward Observatory, University of Arizona, 933 North Cherry Avenue, Tucson, AZ 85721, USA

e-mail: pgperez@; ktyler@; griek@as.arizona.edu

<sup>3</sup> Osservatorio Astronomico di Bologna, via Ranzani, 1 - 47 Bologna - Italy e-mail: olivier.ilbert1@bo.astro.it

<sup>4</sup> California Institute of Technology, MC 405-47, 1200 E. California Boulevard, Pasadena, CA 91125, USA e-mail: tab@srl.caltech.edu

<sup>5</sup> Center for Astrophysical Sciences, The Johns Hopkins University, 3400 North Charles St., Baltimore, MD 21218, USA e-mail: bianchi@skyrv.pha.jhu.edu

<sup>6</sup> Center for Space Astrophysics, Yonsei University, Seoul 120-749, Korea e-mail: ywlee@; yi@galaxy.yonsei.ac.kr

<sup>7</sup> Observatories of the Carnegie Institution of Washington, 813 Santa Barbara Street, Pasadena 91101, USA e-mail: barry@ipac.caltech.edu

<sup>8</sup> NASA/IPAC Extragalactic Database, California Institute of Technology, Mail Code 100-22, 770 S. Wilson Ave., Pasadena, CA 91125, USA

<sup>9</sup> Department of Physics and Astronomy, Johns Hopkins University, 3400 North Charles Street, Baltimore, MD 21218, USA e-mail: szalay@tardis.pha.jhu.edu

<sup>10</sup> Present address: Astronomical Institute, Tohoku University Aoba, Aramaki, Aoba-ku, Sendai 980-8578, Japan e-mail: szalay@tardis.pha.jhu.edu

Received ; accepted

## ABSTRACT

Aims. We present the first large, unbiased sample of Lyman Break Galaxies (LBGs) at  $z \sim 1$ . Far ultraviolet-dropout (1530 Å) galaxies in the Chandra Deep Field South have been selected using GALEX data. This first large sample in the  $z \sim 1$  universe provides us with a high quality reference sample of LBGs.

Methods. We analyzed the sample from the UV to the IR using GALEX, SPITZER, ESO and HST data.

Results. The morphology (obtained from GOODS data) of 75% of our LBGs is consistent with a disk. The vast majority of LBGs with an IR detection are also Luminous Infrared Galaxies (LIRGs). As a class, the galaxies not detected at 24  $\mu$ m are an order of magnitude fainter relative to the UV compared with those detected individually, suggesting that there may be two types of behavior within the sample. For the IR-bright galaxies, there is an apparent upper limit for the UV dust attenuation and this upper limit is anti-correlated with the observed UV luminosity. Previous estimates of dust attenuations based on the ultraviolet slope are compared to new ones based on the FIR/UV ratio (for LBGs detected at 24  $\mu$ m), which is usually a more reliable estimator. Depending on the calibration we use to estimate the total IR luminosity,  $\tau$ -based attenuations  $A_{FUV}$  are larger by 0.2 to 0.6 mag. than the ones estimated from FIR/UV ratio. Finally, for IR-bright LBGs, median estimated  $\tau$ -based SFRs are 2-3 times larger than the total SFRs estimated as  $SFR_{TOT} = SFR_{UV} + SFR_{IR}$  while IR-based SFRs provide values below  $SFR_{TOT}$  by 15 - 20%. We use a stacking method to statistically constrain the 24  $\mu$ m flux of LBGs non individually detected. The results suggest that these LBGs do not contain large amounts of dust.

Key words. cosmology: observations { galaxies: starburst { ultraviolet: galaxies { infrared: galaxies { galaxies: extinction

## 1. Introduction

Lyman Break Galaxies (LBGs) are the most numerous objects observed at high redshift ( $z > 2-3$ ) in the rest-frame

ultraviolet (UV). The discovery of a large population of LBGs beginning with the work of Madau et al. (1996), followed by the spectral confirmation of their redshifts, provided the astronomical community with the first large sample of confirmed high redshift galaxies (Steidel et al. 1996; Lowenthal et al. 1997). The spectra of bright LBGs (e.g. CB58 by Pettini et al. 2000; Teplitz et al. 2000) are remarkably similar to those of local starbursts, indicating that these objects are forming stars at a high rate. The observed colors of LBGs are redder than expected for dust-free star-forming objects. This reddening suggests that some dust is present in this population. However, the amount of dust in LBGs (Baker et al. 2001; Chapman et al. 2000), and therefore the reddening-corrected star formation rate ( $SFR^{\odot}$ ), is poorly known. Meurer et al. (1999), Adelberger & Steidel (2000) and subsequent papers tried to estimate the amount of dust attenuation from the  $\tau$  method (Calzetti et al. 1994). However, it has been shown recently that this approach only provides rough estimates of the total UV attenuation in local galaxies (e.g. Buat et al. 2005; Burgarella et al. 2005; Seibert et al. 2005, Goldader et al. 2002 and Bell 2002).

High redshift LBGs are mainly undetected at submillimeter (sub-mm) wavelengths, where the emission of galaxies is dominated by the dust heated by young stars (Kennicutt 1998). Only the most extinguished LBGs are detected by SCUBA (Chapman et al. 2000, Ivison et al. 2005) and we have no idea of the dust attenuation for a representative sample. Very recently, Huang et al. (2005) observed a population of LBGs at  $2 < z < 3$  detected with SPITZER. Unfortunately, due to the very high redshift, the SPITZER-MIPS observations were not deep enough to detect the thermally reradiated emission from very many LBGs at  $z \sim 3$  and the SPITZER-IRAC data, although deep enough to detect many LBGs, only probe the rest-frame NIR (i.e. no information about the dust enshrouded star formation can be inferred). The morphology of LBGs is also a matter of debate: early works (e.g. Gialalisco et al. 1996) suggested that LBGs could be ellipsoidal, and therefore perhaps the progenitors of ellipticals or of the bulges of spiral galaxies. The problem is that we can hardly detect low surface brightness areas at high redshift because of the cosmological dimming. For instance, Burgarella et al. (2001) suggest that only compact star-forming regions could be easily detected in deep HST observations.

On the other hand, observations in the sub-mm range have revealed a population of FIR-bright galaxies that might be similar to local (Ultra) Luminous IR galaxies ((U)LIRGs) (Blain et al. 1999) with  $10^{11} L_{\odot} < L_{IR} = L(8-1000 \mu m) < 10^{12} L_{\odot}$  for LIRGs and  $10^{12} L_{\odot} < L_{IR} < 10^{13} L_{\odot}$  for ULIRGs. These objects are likely to dominate the Cosmic Infrared Background (CIB; Elbaz & Cesarsky 2003) at high redshift. The link between LBGs and LIRGs is still an open question: are there two classes of objects or are they related? If they are two facets of the same population, then we could, for instance, correct UV fluxes

for the dust attenuation to recover the full Star Formation Density (e.g. Perez-Gonzalez et al. 2005).

The usual way of detecting and identifying LBGs is through the so-called dropout technique, i.e. the absence of emission in the bluest of a series of bands due to the Lyman break feature moving redwards with the redshift (e.g. Steidel & Hamilton 1993, Gialalisco 2002). However, it is well known that selection effects can have a very strong influence on the deduced characteristics of an observed galaxy sample (e.g. Buat et al. 2005; Burgarella et al. 2005). Until now, there has been no way to detect a general, unbiased sample of LBGs at low redshift (i.e.  $z \sim 2$ ), with the same dropout method very successfully used at  $z \sim 2$  because we lacked an efficient observing facility in the UV range. This was quite unfortunate because the simple fact that the galaxies are closer to us means that we can access much more information on the morphology, detect fainter LBGs in the UV and in the IR, and therefore harvest larger samples. GALEX and SPITZER changed this situation and have allowed us to define a large sample of LBGs at  $z \sim 1$  in the Chandra Deep Field South (CDFS).

In this study, we combine the detection in the UV of true (i.e. with a detected Lyman break) LBGs at  $z \sim 1$  with GALEX and at 24  $\mu m$  with SPITZER/MIPS. These data let us estimate the total dust emission and therefore, the dust-to-UV flux ratio, which provides a good tracer of the dust attenuation in the UV. We also use high spatial resolution images to analyse their morphology. We are therefore able to perform a complete analysis for the first time on a large LBG sample.

A cosmology with  $H_0 = 70 \text{ km s}^{-1} \text{ Mpc}^{-1}$ ,  $\Omega_M = 0.3$  and  $\Omega_{\Lambda} = 0.7$  is assumed in this paper.

## 2. The Galaxy Sample

GALEX (Martin et al. 2005) observed the CDFS field for 44668 sec (Deep Imaging Survey = DIS) in both the far ultraviolet (FUV) and the near ultraviolet (NUV). The GALEX field is centered at  $\alpha = 03h32m30.7s$ ,  $\delta = -27deg52'16.9''$  (J2000.0). The GALEX IR1.1 pipeline identified 34610 objects within the  $1.25^\circ$ -diameter field of view. The GALEX resolution (image full width at half Maximum = FWHM) is about 4.5 arcsec in FUV and 6 arcsec in NUV.

This field has also been observed by SPITZER using MIPS (Rieke et al. 2004) in the guaranteed time observing program. The MIPS observations provide about 7-8 sources arcmin<sup>2</sup> at 24  $\mu m$  centered on a  $1.45 \times 0.4 = 0.6 \text{ deg}^2$  field of view. The SPITZER image FWHM is about 6 arcsec and almost perfectly matches that of GALEX.

Redshifts from GOODS (Vanzella et al. 2005) and VVDS (Le Fevre et al. 2004) are available at the center of the GALEX field. Part of the GALEX CDFS field was observed by COMBO 17 (Wolf et al. 2004) over  $0.5 \times 0.5 \text{ deg}^2$ . We made use of COMBO 17 redshifts for objects with  $r < 24.5$ . In this range, the quality

$z = (1+z)$  remains within  $z < 0.03$  for 53 % of the objects. Finally, we obtained photometry from the European Southern Observatory Imaging Survey (EIS) in U, B, V, R and I.

We built a sample of LBGs as follows. From the sources with redshifts, we selected objects in the rest-frame FUV (i.e. in the observed NUV) that we cross-correlated ( $r = 1$  arcsec) first with the ground-based optical EIS data, then ( $r = 4$  arcsec) with the MIPS 24  $\mu$ m data. In the resulting catalogue, we down-selected to objects that COMBO 17 puts in the "GALAXY" class. Then, we extracted the sources with redshift  $0.9 < z < 1.3$ . Since we wish to study Lyman break galaxies, we omitted objects without observed NUV and UV flux: we kept only objects down to GALEX NUV magnitude = 24.5 corresponding to the GALEX 80% completeness level and the U-band limiting magnitude at  $U = 25.1$ . We did not use a color-color selection as performed by Steidel & Hamilton (1993). Since we are studying galaxies with known redshifts, the extra color is not needed to screen out interlopers. The selection on the x-axis (i.e. GR color) might bias the sample toward low-reddening LBGs that we wish to avoid so we can achieve a more general understanding of the sample. In fact, we find that the members of our sample fall within the traditional color-color LBG range, or very close to it, as discussed in Section 3.5. For galaxies at  $z \sim 1$ , GALEX FUV corresponds to a rest-frame wavelength of 765 Å and GALEX NUV corresponds to 1155 Å. The observed FUV and NUV filters are therefore in the same rest-frame wavelength ranges as U and G filters used to identify Lyman breaks at high redshift (e.g. Giavalisco 2002 for a review). The observed FUV-NUV color thus gives a clear indication of the Lyman break. We picked the objects with the strongest indication of a break:  $FUV - NUV > 2$ ; the final sample contains 297 LBGs. Of this list, 49 objects (16.5 %) have a measured flux above the 80% completeness limit of the SPITZER 24  $\mu$ m data (e.g. Perez-Gonzalez et al. 2005) and thus at a high enough ratio of signal to noise to be treated individually. Fig. 1 shows two examples of these LBGs at several wavelengths including the two GALEX bands, the B and R EIS bands and the 24  $\mu$ m SPITZER=MIPS band. Many additional galaxies were detected by SPITZER but at a weaker level; below we will describe how we used a stacking technique to probe their properties. Our sample of 297 UV-selected LBGs in the redshift range  $0.9 < z < 1.3$  constitutes the database that we will study in this work (except for Sect. 3.5). The common GALEX-SPITZER=MIPS-COMBO 17 field of view (mainly limited by COMBO 17) is about  $0.25 \text{ deg}^2$ , which translates to  $\sim 1180 \text{ LBG s deg}^{-2}$  and  $\sim 200 \text{ LBG s deg}^{-2}$  for which we have individual IR detections.

### 3. Lyman Break Galaxies at $z \sim 1$

Our LBGs provide the first opportunity to study an unbiased sample of LBGs systematically at  $z \sim 1$ . We analyze the UV and IR luminosities of these galaxies, measure

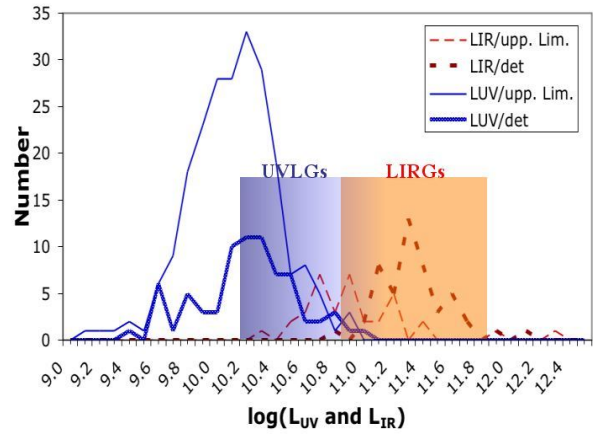


Fig. 2. The distribution in observed luminosity presented here corresponds to UV luminosities in blue (solid) and IR luminosities in red (dashed). Heavy lines are drawn from the population of LBGs with detected counterparts in the 24  $\mu$ m MIPS image and thin lines to upper limits only. Note that the cut at low  $L_{IR}$  is not sharp because the 83 Jy limit used here is not the detection limit but the 80% completeness limit. UV luminosities cover the same range for the two samples and reach uncorrected UV luminosities of  $\text{Log}L_{UV} = 11$  ( $\text{in } L_{\odot}$ ). This upper limit is consistent with Adelberger & Steidel range for LBGs at  $z \sim 3$  but seems inconsistent with the Balmer-break sample at  $z \sim 1$ . Two areas are shaded. Starting from the left, the first corresponds to the range covered by UV Luminous Galaxies (open right ended) and the second one corresponds to Luminous IR Galaxies. A few Ultra Luminous IR Galaxies are also detected.

their morphologies and their star formation as revealed by the UV and IR data and finally discuss the implications they have for studies centered on higher redshifts.

#### 3.1. Ultraviolet and Infrared Luminosities

We find a large range of observed (i.e. un-corrected for dust attenuation) FUV luminosities (in rest-frame FUV) with  $9.3 < \text{Log}L_{UV} [L_{\odot}] < 11.0$ . The lowest luminosity is set by the limiting magnitude in the U-band at  $U = 25.1$ . Below the break, the limiting magnitude amounts to  $FUV = 26.0$ . Although fainter objects are detected in the NUV (down to  $NUV = 25.9$ ), we use a limiting magnitude of  $NUV = 24.5$  to compute safer FUV-NUV colors and therefore perform a safer Lyman Break selection. The average value is  $\langle \text{Log}L_{UV} [L_{\odot}] \rangle = 10.2 \pm 0.3$  for the sample with individual IR detections, and  $\langle \text{Log}L_{UV} [L_{\odot}] \rangle = 10.1 \pm 0.3$  for the rest of the sample.

Total IR luminosities ( $L_{IR}$ ) are estimated following the procedure described in Perez-Gonzalez et al. (2005). Briefly, rest-frame 12  $\mu$ m fluxes are calculated by comparing the observed mid-IR SEDs (including IRAC and MIPS fluxes) of each individual galaxy with models of dust emission (e.g. Chary & Elbaz 2001 or Dale et al.

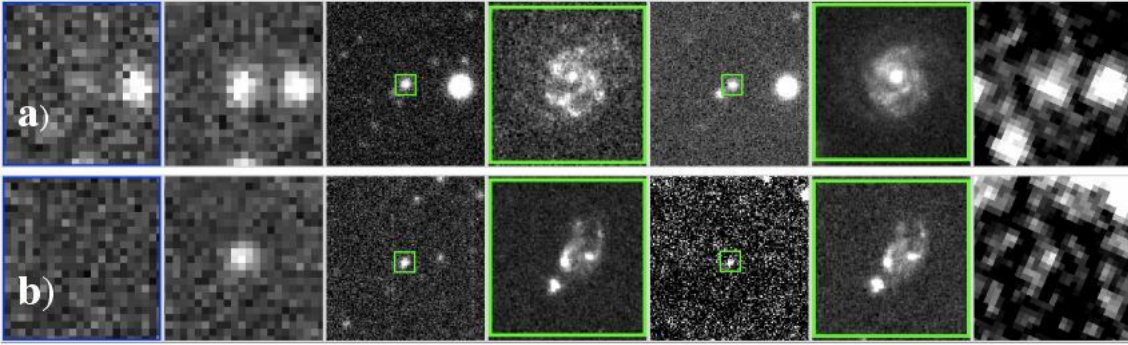


Fig. 1. Two galaxies from our LBG sample are shown here, from left to right in GALEX FUV and NUV, then EIS B, HST GOODS B, EIS I, HST GOODS I and finally SPITZER MIPS 24  $\mu$ m band. For the two galaxies, the leftmost image (blue frame) is below the Lyman break at  $z \sim 1$  and the galaxy is not visible. The size of GOODS images is  $4 \times 4$  arcsec<sup>2</sup>. The corresponding GOODS field (green frame) is plotted in the large ( $35 \times 35$  arcsec<sup>2</sup>) EIS images. a) a LBG classified as a disk-dominated galaxy; the more compact object is at  $z = 0.546$  from VVDS, it appears reddish and should not contribute in ultraviolet and in far infrared; b) a LBG classified as a merger / interacting galaxy.

2002). This procedure is meant to cope with the strong K-corrections observed in the mid-IR due to the emission from aromatic molecules. We use the formulations of Takeuchi et al. (2005) and Chary & Elbaz (2001) for conversion from 12  $\mu$ m flux density to  $L_{\text{IR}}$ . In addition to the intrinsic differences due to the two calibrations (the former provides  $L_{\text{IR}}$  lower by 0.2 dex), the conversion from  $L_{12 \mu\text{m}}$  to  $L_{\text{IR}}$  can introduce errors up to a factor of 2 for individual normal galaxies and 4 for galaxies with SED variations over the full IRAS sample range (Takeuchi et al. 2005; Dale et al. 2005). The effects of these errors are greatly reduced in this work because we discuss average properties, not those of individual galaxies; in this case, the uncertainties are likely to be commensurate with those in the overall conversions to  $L_{\text{IR}}$  (i.e., still 0.2 dex). There are also uncertainties in the luminosity values due to the distance (since we use photometric redshifts with  $z = (z + 1) \pm 0.03$ ), but they are less than 10% for  $L_{\text{UV}}$  and  $L_{\text{IR}}$ .

It is difficult to compare our sample to previously published ones since none was available in this redshift range before GALEX. However, Adelberger & Steidel (2000) have discussed a Balmer-break sample at  $z \sim 1$ . The distributions in  $L_{\text{UV}}$  and  $L_{\text{IR}}$  for our sample are shown in Fig. 2. The lower limit is set by the flux limits but the upper limit of our LBG sample is about the same as the  $z > 3$  one in Adelberger & Steidel's (2000). However, the upper limit of our sample is higher by a factor of 4 (assuming  $H_0 = 70$ ) than Adelberger & Steidel's (2000) sample.

Heckman et al. (2005) defined UV Luminous Galaxies (UVLGs) as galaxies with UV luminosities above  $\text{Log}(L_{\text{UV}}) = 10.3 L_{\odot}$ . They found that these UVLGs bear similarities to LBGs, especially a sub-sample of compact ones. In our sample, 22.2% of the LBGs are UVLGs, 30.6% of the LBGs with an IR counterpart are UVLGs. The 83 Jy detection limit at 24  $\mu$ m approximately corresponds

to  $\text{Log}(L_{\text{IR}}) \sim 11 L_{\odot}$ , that is, nearly all the IR-detected LBGs are LIRGs (95.9%) and there are 2 ULIRGs (4.1%). An association between UVLGs and LIRGs was proposed by Burgarella et al. (2005). We confirm here this association and extend it to LBGs.

### 3.2. The Morphology

The Great Observatories Origins Deep Survey (GOODS) provides high resolution and high signal-to-noise images of some of our LBGs, which can be used to study their morphology in the rest-frame B band. An advantage of our low redshift sample of LBGs is that the images extend to low surface brightness and hence morphologies can be determined well. We compute the asymmetry and concentration (Fig. 3) as in Lauger et al. (2005a) from the objects within the GOODS field which have a signal-to-noise ratio larger than  $S/N \sim 1$  per pixel and whose coordinates are within 2 arcsecs from the GALEX detection. We were able to obtain the morphology for only 36 LBGs out of our 300 LBGs (about 1/4 of our GALEX + SPITZER + COMBO 17 field is covered by GOODS). Fig. 3 leads us to two conclusions: i) all but one LBG in our sample are located on the disk side of the line separating disk-dominated and bulge-dominated galaxies, and ii) part of them (22%) are in the top part of the diagram, i.e. with an asymmetry larger than 0.25 and could be interpreted as mergers. This kind of quantitative analysis is also applied to higher redshift LBGs, however, we must be careful in the interpretation because, even if disks are present, it would be very difficult to detect them due to the cosmological dimming (e.g. Burgarella et al. 2001). Indeed, in deep spectroscopic observations (e.g. Moorwood et al. 2000, Pettini et al. 2001), the profiles of the optical nebular lines suggest the presence of disks in some LBGs.

A number of studies have been devoted to galaxy morphology in the redshift range  $0.6 < z < 1.2$ . At  $z \sim 0.7$ ,

most of the works seem to agree that about 60 – 70% of the objects can be classified as disk-dominated galaxies (mainly spirals and Magellanic irregulars) and 10 – 20% as mergers/interacting galaxies. Here spirals are a sub-group of disks which exhibit a more symmetric (spiral) structure than irregular-like objects similar to the Magellanic clouds. Their asymmetry is therefore lower. Lauger et al. (2005b) found about 70 – 80% of disk-dominated galaxies at  $z \sim 1$ . Zheng et al. (2004) studied the HST morphology of a sample of LIRGs and also found that a large majority (85%) of them are associated with disk-dominated galaxies. This conclusion is reached whether the selection is in the rest-frame ultraviolet (Wolf et al. 2005) or in the infrared (Bell et al. 2005). However, some dispersion due to the cosmic variance might exist (Conselice, Blackburne & Papovich 2005).

Therefore, overall it appears that the majority of the star formation at  $0.6 < z < 1$  resides in disks and about half of it in spirals. The numbers that we draw for our LBG sample at  $z \sim 1$  are globally consistent: we find that 22% of the LBGs are likely mergers (e.g. Fig. 1b),

75% are disks (e.g. Fig. 1a) and only 3% (i.e. 1 galaxy) is possibly a spheroid. In the cases where our LBGs can also be classified as LIRGs from their IR luminosity, our measured morphologies are consistent with the LIRG morphology measurements of Zheng et al. (2004).

### 3.3. Ultraviolet Dust Attenuations

Until now, it has been difficult to estimate the validity of dust attenuation estimates for distant LBGs, because we had no clear idea of their  $L_{\text{IR}}$ . Adelberger & Steidel (2000) tried to estimate the 800  $\mu\text{m}$  fluxes of their LBG sample from the  $\tau_{22}$  method and compared the results to observations. However, only the most extreme LBGs can be detected either directly in the submillimeter range or in the radio range at 1.4 GHz and therefore could be used in this comparison.

In this paper, we use total IR luminosities,  $L_{\text{IR}}$ , and  $L_{\text{UV}}$  to compute the FIR/UV ratio, which is calibrated into FUV dust attenuation  $A_{\text{FUV}}$  (e.g. Burgarella et al. 2005). This method has been shown to provide more accurate dust attenuations than those from the UV slope. Fig. 4 shows an apparent anti-correlation of  $A_{\text{FUV}}$  with the UV luminosity. It is not clear, however, whether this relationship is real or only observational. Indeed, in addition to the observational cut at low  $L_{\text{FUV}}$ , the 24  $\mu\text{m}$  lower limiting flux means that we cannot detect individually low-luminosity galaxies with low dust attenuations. It is very interesting to note that we do not detect LBGs with both a high UV luminosity and a high UV dust attenuation, and this cannot be caused by observational limits. In other words, we seem to observe a population of high  $L_{\text{UV}}$  LBGs (which qualify as UVLGs) with dust attenuations similar to UV-selected galaxies in the local universe (e.g. Buat et al. 2005). UVLG galaxies are LIRGs with the lowest  $A_{\text{FUV}}$ .

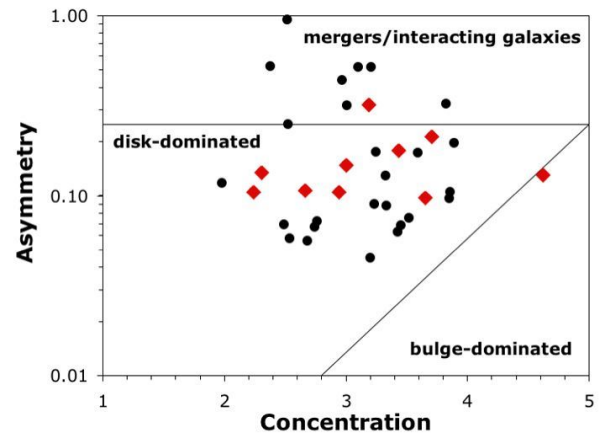


Fig. 3. The morphology of the LBG sample is quantitatively estimated from the asymmetry and the concentration (sub-sample drawn from a larger CDFS analysis by Lauger et al. 2005b). The smaller number of objects presented here is due to the smaller field of view of GOODS as compared to ours. Black circles are LBGs without IR counterparts while red diamonds represent LBGs with a 24  $\mu\text{m}$  MIPS detection. The line corresponding to the limit between disk-dominated and bulge-dominated galaxies (Lauger et al. 2005a). The location in the diagram reflects the morphological type of the galaxies: more asymmetrical LBGs (e.g. mergers) are in the top part of the diagram ( $A > 0.25$ ) while early-type spirals would have  $A < 0.1$ . The LBG sample is mainly dominated (75%) by disk-dominated galaxies and the contribution from mergers amounts to 21%.

There are now studies of high-redshift LBGs ( $z > 2$ ) with SPITZER (e.g. Labbé et al. 2005; Huang et al. 2005). However, the results are so far inconsistent: Labbé et al. (2005) found that LBGs are consistent with low-reddening models while Huang et al. (2005) found more reddened LBGs. Further observations will resolve these differences and provide a firm basis for comparison with our sample.

With the 24  $\mu\text{m}$  SPITZER flux for the individually detected  $z \sim 1$  objects, we can go a step further and check how UV dust attenuation estimations carried out from the  $\tau_{22}$  method compare with the better IR=UV-based estimates. This comparison has already been performed for nearby galaxies (Buat et al. 2005, Burgarella et al. 2005, Seibert et al. 2005 and references therein). Given the wide use of the  $\tau_{22}$  method on high redshift LBGs, it is useful to compare with our lower-redshift sample.

Using the equations in Adelberger & Steidel (2000) (deduced from Meurer et al. (1999)), we estimate the IR luminosity that is used to compute  $A_{\text{FUV}}$  and the total luminosity for each LBG. We observe a small overestimation of the dust attenuation as compared to the ones estimated from SPITZER=MIPS data and the dust-to-UV flux ratio. The  $\tau_{22}$ -based mean dust attenuation estimated for our  $z \sim 1$  LBG sample is  $A_{\text{FUV}} = 2.76 \pm 0.13$ .

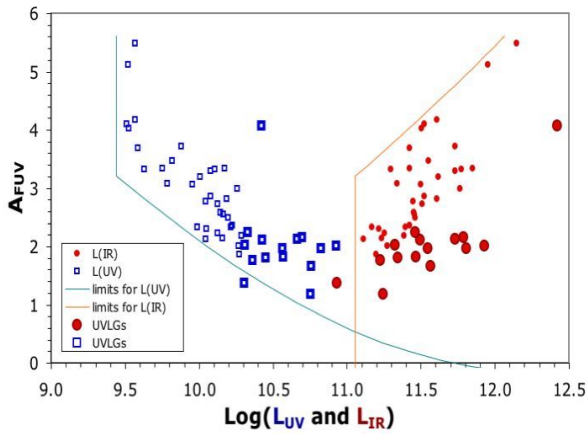


Fig. 4. Blue and red symbols are the same objects but luminosities are  $L_{UV}$  for the former and  $L_{IR}$  for the latter. The dust attenuation strongly decreases while  $L_{UV}$  increases. Part of this apparent correlation might be due to the fact that observational limits prevent us from detecting low-luminosity LBGs with low dust attenuation. The clear cut on the upper parts of the box cloud cannot be due to observational biases. We do not seem to observe UVLGs with high dust attenuations. On the other hand, the more dispersed but well-known increase of the dust attenuation with  $L_{IR}$  is observed here. Larger symbols correspond to UVLGs ( $\text{Log} L_{UV} > 10.3L_{\odot}$ ). Most of them have low dust attenuations but one is a ULIRG and has  $A_{FUV} \sim 4$ .

( $\sigma = 1.02$ ) while the dust-to-UV dust attenuation gives  $A_{FUV} = 2.16 \pm 0.11$  ( $\sigma = 0.84$ ) with  $L_{IR}$  from Takeuchi et al. (2005) and  $A_{FUV} = 2.53 \pm 0.12$  ( $\sigma = 0.94$ ) with  $L_{IR}$  from Chary & Elbaz (2001). The average value of the two dust-to-UV estimates is consistent with Takeuchi, Buat & Burgarella (2005). The net effect is that total luminosities based on the  $\beta$  method are slightly larger than the actual values and the deduced SFRs are therefore overestimated (see next section). The mean of the ratios of the FIR/UV  $A_{FUV} = 1.31 \pm 0.07$  ( $\sigma = 0.52$ ) for Takeuchi et al. (2005) and  $A_{FUV} = 1.09 \pm 0.05$  ( $\sigma = 0.40$ ) for Chary & Elbaz's calibration.

Applying the Kaplan-Meier estimator (and using Chary & Elbaz's calibrations), we can take upper limits into account to estimate mean dust attenuations. We find moderate values  $\langle A_{FUV} \rangle = 1.36 \pm 0.07$  for  $M_{FUV} < -22$  (5 data points of which 1 is an upper limit) and  $\langle A_{FUV} \rangle = 1.08 \pm 0.11$  for  $M_{FUV} < -21$  i.e.  $L_?$  at  $z=3$  (35 data points of which 65% are upper limits). Using only detections, we reached, respectively,  $\langle A_{FUV} \rangle = 1.54 \pm 0.09$  and  $\langle A_{FUV} \rangle = 1.59 \pm 0.18$ . Since we only use a small number of bright LBGs, this is hardly comparable to the numbers quoted in the previous paragraph. However, it suggests that lower  $L_{FUV}$  LBGs have higher dust attenuations (see Fig. 4).

### 3.4. Star Formation Rates and Implications for the Cosmic Star Formation Density

We estimate SFRs for our LBG sample from the IR luminosities and after applying dust corrections estimated from  $\beta$  and we compare them, in Fig. 5, to the total SFR:  $\text{SFR}_{TOT} = \text{SFR}_{UV} + \text{SFR}_{IR}$  where  $\text{SFR}_{UV}$  is not corrected for dust attenuation.  $\text{SFR}_{TOT}$  is assumed to be the best SFR estimate and we use it as a reference. The first conclusion is that the dispersion is much larger for UV SFRs computed with dust corrections than for IR SFRs. But the median values are also different:  $\text{SFR}_{UV}^C = 112.3 \pm 33.8$  ( $\sigma = 260.9$ )  $M_{\odot} \text{yr}^{-1}$  while  $\text{SFR}_{IR} = 49.9 \pm 13.1$  ( $\sigma = 100.9$ )  $M_{\odot} \text{yr}^{-1}$  if we use Chary & Elbaz (2001) and  $\text{SFR}_{IR} = 30.5 \pm 6.0$  ( $\sigma = 46.6$ )  $M_{\odot} \text{yr}^{-1}$  if we use Takeuchi, Buat & Burgarella (2005). Median  $\text{SFR}_{TOT}$  for the two above calibrations are, respectively,  $\text{SFR}_{TOT} = 62.8 \pm 13.2$  ( $\sigma = 102.1$ )  $M_{\odot} \text{yr}^{-1}$  and  $\text{SFR}_{TOT} = 41.1 \pm 6.3$  ( $\sigma = 48.6$ )  $M_{\odot} \text{yr}^{-1}$ . As expected, for LBGs detected in IR,  $\text{SFR}_{IR}$  is therefore a better estimate. About 22% of our LBGs with an IR detection have  $\text{SFR}_{TOT} > 100 M_{\odot} \text{yr}^{-1}$  (using Chary & Elbaz's calibration) as compared to less than 1% in Flores et al.'s (1999) galaxy sample which confirms that our LBGs are forming stars very actively. However, none of the LBGs undetected at 24  $\mu\text{m}$  is above  $\text{SFR}_{TOT} > 100 M_{\odot} \text{yr}^{-1}$ .

The higher SFRs reached when dust attenuations are computed with the UV slope (depending on the  $L_{IR}$  calibration, +79 to +173%) lead to an overestimated contribution of LBGs to the Cosmic Star Formation Density if the same quantitative difference exists at higher redshift. However, Takeuchi, Buat & Burgarella (2005) showed that the current assumption of a constant dust attenuation does not seem to be verified. The increase of the mean  $A_{FUV}$  from 1.3 to 2.3 from  $z = 0$  to  $z = 1$  means that, for a given observed FUV luminosity density, the dust-corrected star formation density would vary. Note that those mean dust attenuations cannot be compared with the numbers given for the Kaplan-Meier estimates which are biased toward large  $M_{FUV}$  LBGs while fainter LBGs seem to have larger dust attenuations in our sample. Although FIR data are not always available, it is very important that one is aware of these uncertainties when using Star Formation Densities derived from UV values corrected from the  $\beta$  method for LBGs with high dust attenuations, especially at high redshift where we have a very poor knowledge of actual attenuations. These ambiguities may be reduced by further study of Spitzer data, and with Herschel.

### 3.5. Extension to Galaxies Faint at 24 $\mu\text{m}$

So far, most of our arguments have been based on the 49 galaxies individually detected at 24  $\mu\text{m}$  well above the completeness limit. To put the behavior of these galaxies in a broader context, we have determined average infrared flux densities for groups of galaxies by stacking. Images at 24  $\mu\text{m}$  are shifted to a common center on the basis of the

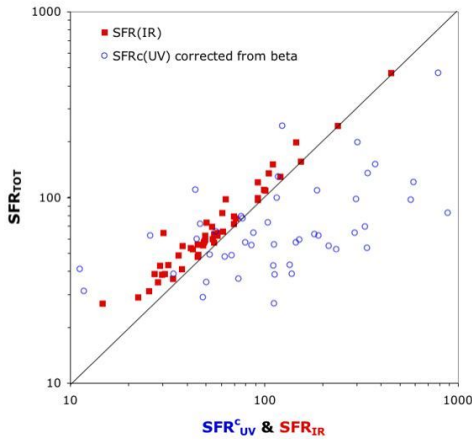


Fig. 5. Blue open circles compare  $SFR_{UV}^C$  to  $SFR_{TOT}$  while red filled boxes compare  $SFR_{IR}$  to  $SFR_{TOT}$ . Both SFRs are computed from Kennicutt (1998). The median  $SFR_{IR}$  is underestimated by about 80% and the underestimation increases at lower SFRs, which is consistent with the fact that the UV contribution (not accounted for from  $L_{IR}$ ) is usually higher at low SFRs than at high SFRs. For this sample of LBG detected at 24  $\mu\text{m}$ , the median value of  $SFR_{UV}^C$  is overestimated by a factor of 2–3 in average with a possible trend for the difference to increase at high SFRs. The dispersion of  $\beta$ -based UV SFRs ( $SFR \sim 200 M_{\odot} \text{ yr}^{-1}$ ) is much larger than IR-based SFR ( $SFR \sim 30\text{--}40 M_{\odot} \text{ yr}^{-1}$  depending on the calibration into  $L_{IR}$ ).

24  $\mu\text{m}$  coordinates if the object was well enough detected in that band, or the coordinates of the optical identification otherwise. We use sigma-clipping to eliminate surrounding sources; the level at which clipping occurs is adjusted empirically to provide the smoothest possible sky image. The quoted results are for a level of 5 $\sigma$  for sources detected at 24  $\mu\text{m}$  and 4 $\sigma$  for undetected ones (see below), but they are not sensitive to modest adjustments in this level. In general, the resulting backgrounds have only weak structure and, where the sources are fairly bright in the infrared, the 24  $\mu\text{m}$  stacked image is similar to the point spread function of the instrument. We confirmed that stacking sources of known flux density gave consistent results. These behaviors validate the procedure.

For this study, we used a total of 336 sources, selected similarly to those discussed above (but without screening for COMBO-17 type classification). We divided the sample into two groups. The first, hereafter the undetected group, includes 201 UV objects (60% of the total) for which visual inspection indicated no reliable 24  $\mu\text{m}$  detection. The second (40%), hereafter the detected group, is the objects with evidence for an infrared detection; it was in turn divided into three equal subgroups according to NUV luminosity. As shown in Table 1, the two groups have very similar average NUV flux density, 1.89 Jy for the undetected and 1.63 Jy for the detected group. The average NUV luminosities are also similar,  $1.3 \times 10^{44}$  erg/s

and  $1.1 \times 10^{44}$  erg/s, respectively. However, the average infrared flux densities differ by a factor of ten: 13 Jy for the undetected group and 143 Jy for the detected one. There is no significant difference in average infrared flux density among the subgroups in the detected group.

These results indicate that the LBGs divide into two classes. About 40% of them are infrared bright. The average NUV flux density for this group is 1.63 Jy, so as measured in F, the NUV and 24  $\mu\text{m}$  luminosities are similar. Since there is a substantial correction to total far infrared luminosity, the infrared component to the output from young stars is significant, probably accounting for the majority of the luminosity for these objects. The remaining 60% are infrared faint: F is about ten times greater in the NUV than at 24  $\mu\text{m}$ , indicating that their outputs are dominated by the UV. The results of this paper apply to galaxies like those in the detected group only.

To explore other possible differences between these classes, we computed the average B (i.e. rest-frame NUV) flux densities for the same two groups and three subgroups. Although it is influenced by other factors, we take the ratio of B to NUV flux densities (or equivalently the NUV–B color) to be an indicator of the level of reddening, and the ratio of 24  $\mu\text{m}$  to B flux density to measure the relative portion of the luminosity from young stars emerging in the infrared compared with the UV. The results are in Table 1. First, they demonstrate that all the galaxies in our selection fall in, or close, to the color-color LBG zone as adjusted from high  $z$  to  $z \sim 1$  (see Gialalisco 2002). There is a trend for LBGs with a high 24/B ratio to present a high B/NUV, which is consistent with the relation for the UV slope and the FIR/UV ratio found by Meurer et al. (2000) on a sample of local starburst galaxies. An analysis based on detections is required to check whether Meurer et al.’s law can be applied safely to those LBGs while we showed in the previous section that it provides dispersed SFRs for the detected sample. Finally, the amount of dust attenuation for the undetected group is very low ( $A_{FUV} = 0.5\text{--}0.6$  for a mean  $\text{Log} L_{TOT} = 10.5$ ) which corresponds to LBGs with the lowest reddening found by Adelberger and Steidel (2000). This very low reddening is consistent with the very blue UV slope  $\beta = 2.4$ . If confirmed, this would mean that about half of the LBGs do not contain large amounts of dust.

#### 4. Conclusions

We use multi-wavelength data in the CDFS to define the first large sample of Lyman Break Galaxies at  $z \sim 1$ ; GALEX is used to observe the Lyman break. Redshifts are taken from spectra and from COMBO-17. Quantitative morphologies (Lauger et al. 2005a) are estimated from high spatial resolution images. Finally, dust attenuations and total luminosities are computed from SPITZER measurements at 24  $\mu\text{m}$  extrapolated to get the total IR luminosity.

The main results of this analysis are:

Table 1. Stacking Analysis Results

	number	$L_{UV}$ $10^{44}$ ergs/sec	$F(24\text{ m})$ m Jy	$F(B)$ m Jy	$F(NUV)$ m Jy	$F(B)/F(NUV)$	$F(24)/F(B)$
All detected	135	1.11	0.14	0.0018	0.0016	1.11	80
low UV	45	0.67	0.16	0.0014	0.0012	1.21	113
middle UV	45	0.99	0.16	0.0017	0.0014	1.19	95
high UV	45	1.67	0.14	0.0023	0.0024	0.98	59
Undetected	201	1.33	0.013	0.0015	0.0019	0.79	8.7

- We detect LBGs in the range  $9.3 < \text{Log}L_{FUV} [L_{\odot}] < 11.0$ , i.e. well into the UVLG class as defined by Heckman et al. (2005). For the same objects,  $\text{Log}L_{IR} > 11L_{\odot}$ , which means that almost all the LBGs with a SPITZER confirmed detection are LIRGs (and 1 ULIRG) at  $z \sim 1$ .
- LBGs at  $z \sim 1$  are mainly disk-dominated galaxies (75%) with a small contribution of interacting/merging galaxies (22%) and a negligible (3%) fraction are spheroids. The morphologies of our LBG sample are consistent with star-forming galaxies.
- The FUV dust attenuation appears to be anti-correlated with the observed FUV luminosity. Part of this correlation might be due to observational limits at 24 m. However, non-detection of LBG with high  $L_{FUV}$  and high  $A_{FUV}$  cannot be explained by observational biases.
- About 40% of our sample of LBGs is detected at 24 m. These objects also show evidence for reddening in their UV continua. The remaining 60% of the sample are on average an order of magnitude less luminous in the infrared compared with the rest frame near UV. Their UV continua also appear to be significantly less reddened.
- Dust corrections of our IR-bright LBG sample computed via the method are over-estimated by 0.2 mag. if we use Chary & Elbaz (2001) to compute  $L_{IR}$  and by 0.6 mag. if we use Takeuchi, Buat & Burgarella (2005).
- Dust attenuations estimated by the method for such galaxies lead to overestimation of the SFRs at  $z \sim 1$  by a factor of 2 to 3, depending on the calibration of the 24 m flux to  $L_{IR}$  while IR-based SFRs are of the same order as  $SFR_{TOT}$ .
- By using the stacking method, we find that LBGs non detected at 24 m seem to have very low dust attenuations.

Acknowledgements. TTT has been supported by the Japan Society for the Promotion of Sciences (April 2004 – December 2005). Support for this work was provided by NASA through Contract Number 960785 issued by JPL/CALTECH. This work is based on observations made with the Spitzer Space Telescope, which is operated by the Jet Propulsion Laboratory, California Institute of Technology under NASA contract 1407. Analysis of the data for this paper was supported by the contract to the MIPS team, 1255094. We also thank the French Programme National Galaxies and the Programme National Cosmologie for their financial support. We gratefully acknowledge NASA's

support for construction, operation and science analysis for the GALEX mission developed in cooperation with the Centre National d'Etudes Spatiales of France and the Korean Ministry of Science and Technology. Finally, we thank Eméric Le Floch for his help and discussions during this work.

## References

- Adelberger K.L., Steidel C.C. 2000, ApJ, 544, 218  
 Baker A.J., Lutz D., Genzel R., Tacconi L.J., Lehnert M.D., 2001 A & A, 372, 37  
 Bell E.F. 2002 ApJ, 577, 150  
 Bell E.F., Papovich C., Wolf C., Le Floch E., Caldwell J.A.R., Barden M., Egami E., McIntosh D.H., Meisenheimer K., Prez-Gonzalez P.G. et al. 2005 ApJ, 625, 23  
 Blain A.W., Smail I., Ivison R.J., Kneib J.-P., 1999 MNRAS, 302, 632  
 Buat V., Iglesias-Paño J., Seibert M., Burgarella D., Charlot S., Martin D.C., Xu C.K., Heckman T.M., Boissier S., Boselli A. et al., 2005 ApJ, 619, L51  
 Burgarella D., Buat V., Donas J., Miliard B., Chapelon S. 2001 A J, 369, 421  
 Burgarella D., Buat V., Smail T., Barlow T.A., Boissier S., Gildes-Paz A., Heckman T.M., Madore B.F., Martin D.C., Rich R.M. et al., 2005 MNRAS, 360, 1413  
 Calzetti D., Kinney, A.L., Storchi-Bergmann T. 1994, ApJ 429, 582  
 Chapman S.C., Scott D., Steidel C.C., Borys C., Halpern M., Morris S.L., Adelberger K.L., Dickinson M., Gialalisco M., Pettini M. 2000 MNRAS, 319, 318  
 Chary R. & Elbaz D., 2001 ApJ, 556, 562  
 Conselice C.J., Blackburne, J.A., Papovich C., 2005 ApJ 620, 564  
 Dale D.A. et al., 2005 ApJ in press (astro-ph/0507645)  
 Dale D.A., Helou G. 2002 ApJ 576, 159  
 Elbaz D., Cesarsky C.J. 2003 Science 300, 270  
 Flores H., Hammer F., Thuan T.X., Cesarsky C., Desert F.X., Omont A., Lilly S.J., Eales S., Crampton D., LeFevre O., 1999 ApJ 517, 148  
 Gialalisco M., Steidel C.C., Mochetto F.D. 1996 ApJ, 470, 189  
 Gialalisco M. 2002 ARA & A, 40, 579  
 Goldader J.D., Meurer G., Heckman T.M., Sanders D.B., Calzetti D., Steidel C.C. 2002, ApJ 568, 651  
 Heckman T.M., Hoopes C.G., Seibert M., Martin D.C., Salim S., Rich R.M., Kaufmann G., Charlot S., Barlow T.A., Bianchi L. et al. 2005 ApJ 619, L35  
 Huang J.-S. et al., 2005 ApJ in press (astro-ph/0507685)  
 Ivison R.J., Smail I., Bentz M., Stevens J.A., Menendez-Del-Mestre K., Chapman S.C., Blain A.W. 2005 MNRAS 362, 535  
 Kennicutt R.C., 1988 ARA & A 36, 189

- Labbe I., Huang J., Franx M., Rudnick G., Barmby P., Daddi E., van Dokkum P.G., Fazio G.G., Forster Schreiber N.M., Moorwood A.F.M. et al. 2005 ApJ624, L81
- Lauger S., Burgarella D., Buat V. 2005a A & A 434, 77
- Lauger S. et al., 2005b A & A submitted
- LeFevre O., Vettolani G., Paltani S., Tresse L., Zamorani G., Le Brun V., Moreau C., Bottini D., Maccagni D., Picat J.P., et al. 2004 A & A 428, 1043
- Lowenthal J.D., Kooldavid C., Guzman R., Gallego J. Phillips A.C., Faber S.M., Vogt N.P., Illingworth G.D., Gronwall C. 1997 ApJ481, 673
- Madau P., Ferguson H.C., Dickinson M.E., Giavalisco M., Steidel C.C., Fruchter A. 1996 MNRAS, 283, 1388
- Martin D.C., Fanson J., Schiminovich D., Morrissey P., Friedman P.G., Barlow T.A., Conrow T., Grange R., Jelinsky P.N. et al., 2005. ApJ, 619, L1
- Meurer, G.R., Heckman, T.M., & Calzetti, D. 1999, ApJ 521, 64
- Moorwood A.F.M., van der Werf P.P., Cuby J.G., Oлива E. 2000. A & A, 362, 9
- Perez-Gonzalez, P.G. et al., 2005 ApJ in press, (astro-ph/0505101)
- Pettini M., Steidel C.C., Adelberger K.L., Dickinson M., Giavalisco M. 2000 ApJ528, 96
- Pettini M., Shapley A.E., Steidel C.C., Cuby J.G., Dickinson M., Moorwood A.F.M., Adelberger K.L., Giavalisco M. 2001 ApJ554, 981
- Rieke G.H., Young E.T., Engelbracht C.W., Kelly D.M., Low F.J., Haller E.E., Beaman J.W., Gordon K.D., Stansberry J.A., Missett K.A. et al. 2004 ApJS154, 25
- Seibert M., Martin D.C., Heckman T.M., Buat V., Hoopes C., Barlow T., Bianchi L., Byun Y.-I., Donas J., Forster K. et al. 2005 ApJ, 619, L59
- Steidel, C.C. & Hamilton D., 1993 AJ, 105, 201
- Steidel, C.C., Giavalisco, M., Pettini, M., Dickinson, M., & Adelberger, K.L. 1996, ApJ 462, L17
- Teplitz H., McLean I.S., Becklin E.E., Figer D.F., Gilbert A.M., Graham J.R., Larkin J.E., Levenson N.A., Wilcox, M.K. ApJ, 533, 65
- Takeuchi T.T., Buat V., Iglesias-Paramo J., Boselli A., Burgarella D. 2005 A & A, 432, 423
- Takeuchi T.T., Buat V., & Burgarella D. 2005, A & A, 440, L17
- Vanzella E., Cristiani S., Dickinson M., Kuntschner H., Moustakas L.A., Nonino M., Rosati P., Stem D., Cesarsky C., Etori S., et al. 2005 A & A 434, 53
- Wolf C., Meisenheimer K., Kleinheinrich M., Borch A., Dye S., Gray M., Wisotzki L., Bell E.F., Rix H.-W., Cimatti A., et al. 2004 A & A 421, 913
- Wolf C., Bell E.F., McIntosh D.H., Rix H.-W., Barden M., Beckwith S.V.W., Borch A., Caldwell J.A.R., Haussler B., Heymans C., et al., 2005 ApJ630, 771
- Zheng X.Z., Hammer F., Flores H., Assmat F., Pelat D. 2004 A & A 421, 847